PAPER

NJC

www.rsc.org/njc

Computational QM/MM study on the structure and energetics of species involved in the activation of the C–H and C–S bonds of thiophene by Cp*RhPMe$_3$

Olivier Maresca,* Feliu Maseras and Agustí Lledós

Unitat de Química Física, Universitat Autònoma de Barcelona, Edifici C.n,, 08193, Bellaterra, Catalonia, Spain. E-mail: olivier@klingon.uab.es

***Received* (in Montpellier, France) 25th September 2003, Accepted 19th January 2004**
First published as an Advance Article on the web 7th April 2004

The hybrid quantum mechanics/molecular mechanics (QM/MM) method IMOMM is applied to the calculation of the reaction of thiophene with Cp*RhPMe$_3$, which is a good experimental model for homogeneous catalytic hydrodesulfurization (HDS). The validity of the results is checked by comparison with previously reported full QM calculations on the same system. The geometries obtained with IMOMM are in good agreement with those obtained with full QM. Concerning the energies of the reaction path, differences from full QM results are found for steps involving a change in the oxidation state of the Rh atom. The effect of the methyl substituents on each reaction step is quantified and separated into steric and electronic contributions.

Introduction

Sulfur compounds act as poisoning agents on the catalysts used for cracking and reforming of crude petroleum[1] and, furthermore, they are highly contaminant subproducts of fuel combustion involved in atmospheric pollution.[2] Because of this, hydrodesulfurization (HDS), the reaction by which sulfur is removed from crude petroleum and eliminated as hydrogen sulfide, is a process of great industrial importance.[3]

Despite its formal simplicity, the HDS process is accomplished only with difficulty in a number of cases. In particular, compounds in which sulfur is involved in aromatic rings are difficult to desulfurize. This is the case especially for dibenzothiophene and 4,6-dimethyldibenzothiophene.[4–6] The HDS process is usually performed *via* heterogeneous catalysis. A typical combination of catalysts could be, for instance, alumina-supported molybdenum or tungsten catalysts promoted with cobalt or nickel.[1,7] Optimization of this type of catalysts is obviously complicated because of the difficulty in ascertaining their reaction mechanism and is largely based on empirical testing. Certainly, in heterogeneous catalysis, mechanistic studies are difficult and the reactive intermediates between reactants and products can very seldom be characterized. Progress in understanding the coordination mode of thiophene and its derivatives to catalyst surfaces and on the structure of the surface itself is currently being made with the use of both experimental[8–12] and theoretical methods[13–20] but a detailed understanding of the reaction mechanism of heterogeneous HDS appears to be still far in the future.

The difficulty in understanding the mechanism of the industrially useful heterogeneous HDS process fuels interest in research on the homogeneous activation of thiophene and its derivatives by transition metal complexes.[21–23] In a homogeneous process, the reaction is easier to control and follow and the conventional tools of analytical chemistry can be more easily applied. The insights obtained in homogeneous HDS can be subsequently applied to the design of an efficient homogeneous catalyst or to a better understanding of the reaction mechanism of the heterogeneous process.

Organometallic complexes have been shown to be able to coordinate thiophene and their aromatic derivatives and to activate them towards different reactions.[21–29] Probably the most relevant of these reported reactions is the insertion of the metal atom into the C–S bond of thiophene and its derivatives, because the breaking of this bond is a necessary step within the HDS process. This insertion reaction has been documented for a number of mono-[23,28–37] and dinuclear organometallic fragments.[38,39] Of particular interest is the case of rhodium complexes of the Cp*(Me$_3$P)Rh,[30,31,33,40] and Tp*(R$_3$P)Rh,[36] types. In particular, the experimental study by Dong and coworkers[40] and, later, the theoretical study by Sargent and coworkers[41,42] have lead to the definition of the qualitative reaction profile shown in Scheme 1. The reactants, thiophene and Cp*(Me$_3$P)Rh, interact in two different ways: through η^1 coordination of the sulfur atom (intermediate **1**) or through η^2 coordination of two carbon atoms (intermediate **2**). Each intermediate gives rise to a different product involving C–S activation (product **3**) or C–H activation (product **4**).

Calculations are increasingly useful tools in transition metal chemistry.[43,44] Although this reaction could be calculated with an accurate quantum mechanical (QM) method,[42] the size of the systems involved in these processes still poses a challenge

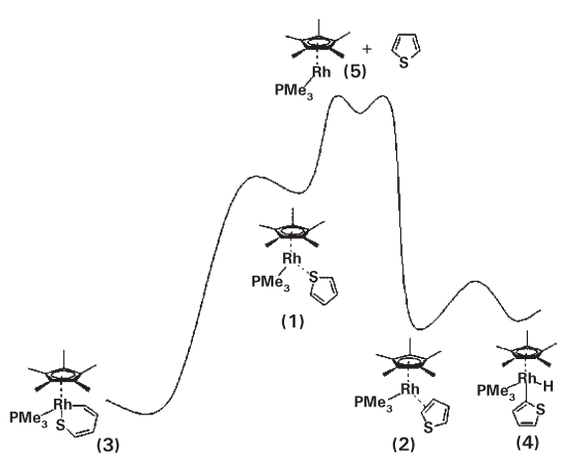

Scheme 1

DOI: 10.1039/b311926b

to current computational resources, especially if sulfur-containing molecules larger than thiophene are to be considered. Because of this, the application of hybrid QM/MM methods, in which a region of the system is treated with a more affordable molecular mechanics (MM) description, looks attractive. In fact, these methods[45] have been applied with success to a variety of problems in transition metal chemistry,[46,47] including a case involving thietane coordination to the metal.[48]

We present in this work a computational study with the hybrid IMOMM method[45] on the reaction of thiophene with Cp^*RhPMe_3. The aim of this work is twofold. On one hand, this is the first attempt to observe the performance of QM/MM methods in the computational modeling of hydrodesulfurization. On the other hand, the ability of the method to separate steric and electronic effects, which has been previously proven,[47,49] will allow a better understanding of the features of the particular process under study. The role of methyl substituents will also be analyzed with the help of this method.

Computational details

Hybrid QM/MM calculations with the IMOMM[45] method were carried out with a program built from modified versions of the standard programs Gaussian 92/DFT[50] and mm3(92).[51] The QM region was $CpRhPH_3$ plus thiophene as shown in Fig. 1.

The quantum calculations were performed at the B3LYP level.[52] The standard effective core potential basis set LANL2DZ was used for the rhodium,[53] sulfur and phosphorus atoms.[54] The associated valence double ζ basis set was used for these atoms. For the carbon and hydrogen atoms, the valence double ζ 6-31G[55] basis set was used. This basis set is very similar in quality to that of Sargent and Titus in their previous computational study.[42] We did not add an additional set of p functions on the Rh because preliminary calculations showed it had little effect on the results.

Molecular mechanics calculations used the MM3 force field with standard parameters.[56] The van der Waals parameters of the rhodium atom were those of the UFF force field.[57] Torsional contributions involving dihedral angles with the metal in the terminal position were set to zero.

Optimizations were full except for the connection between the QM and the MM region where the P–H (1.420 Å) and the C(sp2)–H (1.101 Å) bond lengths in the QM part and the P–C (1.843 Å) and the C(sp2)–C(sp3) (1.499 Å) bond lengths in the MM part were frozen.

Results and discussion

IMOMM optimizations on the full system

Experimental results and previous theoretical calculations indicated the presence of four different species in the reaction between Cp^*RhPMe_3 and thiophene as shown in Scheme 1. These correspond to the η^1 coordination of thiophene, **1**, the η^2 coordination to thiophene, **2**, and the two oxidative addition products, corresponding to C–S activation, **3**, and to C–H activation, **4**. The set of computed local minima was completed with a calculation on the separated reactants, **5**. All these species have been computed with the IMOMM method.

The optimized IMOMM geometries are presented in Fig. 2 and selected geometrical parameters are included in Table 1. Table 1 also includes the full QM results[42] for comparison.

It can be seen that the IMOMM geometries follow faithfully the previously reported trends. The η^1 character of **1** is indisputable from the short Rh–S distance of about 2.4 Å and the two long Rh–C2 and Rh–C3 distances, greater than 3.6 Å. The η^1 coordination does not affect the π system of the thiophene. The S–C2 and S–C5 bond lengths before (**5**) and after (**1**) binding are nearly the same. In complex **2**, the η^2 mode is related to the interaction of the metal center with the π system of the C2 and C3 atoms of the thiophene five-membered ring (**2** in Fig. 2). Here, the Rh–C2 and Rh–C3 distances are short (around 2.15 Å) and the Rh–S is long (around 3.5 Å). Furthermore, C2 and C3 have lost their sp^2 hybridization to become sp^3 carbons. The bonded thiophene molecule is non-planar. The π system is involved in the bonding, the S–C2 and S–C4 bond lengths are different in comparison with those in free thiophene, and a significant lengthening is observed in the case of the C–S and the C–C bonds when going from **5** to **2**.

In the insertion product **3**, the metal is inserted between the C2 and the S atom to form a six-membered ring. The breaking of the bond is complete, as reflected by the S–C2 distance, which is longer than 3.2 Å. In this complex, one must note that the formal oxidation number of the metal is equal to three

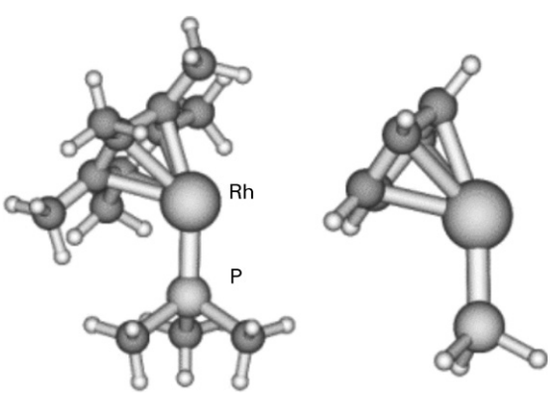

Fig. 1 The full system (left) and the QM region (right) used in the IMOMM calculations.

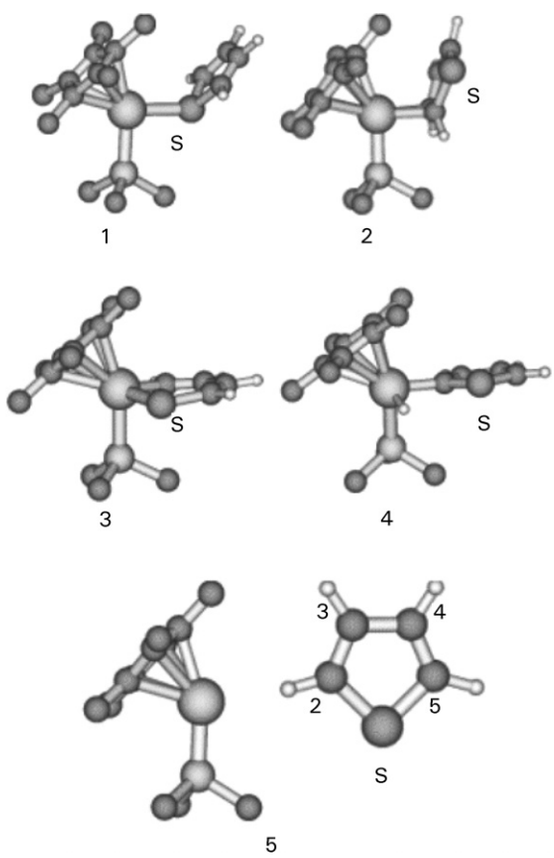

Fig. 2 Optimized IMOMM geometries and atom labelling of the thiophene molecule. The hydrogen atoms of the Cp^*RhPMe_3 complex are omitted for clarity.

Table 1 Selected geometrical parameters (in Å and °) obtained from the IMOMM(B3LYP:MM3) optimization of complexes **1** to **4** and of reactants **5**. Previously reported pure QM values[42] are also presented for comparison. The atom labelling used is defined in Fig. 2

	5		**1**		**2**		**3**		**4**	
	Pure QM	QM/MM	Pure QM	QM/MM	Pure QM	QM/MM	Pure QM	QM/MM	Pure QM	QM/MM
Rh–P	2.335	2.340	2.354	2.353	2.377	2.384	2.366	2.384	2.352	2.358
Rh–S			2.414	2.451	3.482	3.461	2.429	2.438	3.402	3.378
Rh–C2			3.688	3.637	2.124	2.135	2.032	2.031	2.036	2.022
Rh–C3			4.678	4.551	2.186	2.209	3.122	3.098	3.132	3.081
S–C2	1.813	1.802	1.832	1.822	1.887	1.866	3.271	3.235	1.854	1.836
C2–C3	1.392	1.364	1.386	1.358	1.477	1.445	1.381	1.351	1.406	1.377
C3–C4	1.461	1.440	1.468	1.450	1.482	1.462	1.478	1.455	1.465	1.433
C4–C5	1.392	1.364	1.386	1.357	1.380	1.353	1.381	1.350	1.391	1.363
S–C5	1.813	1.802	1.832	1.822	1.836	1.822	1.815	1.803	1.819	1.808
Rh–H			3.951	3.900	2.789	2.746	2.652	2.613	1.561	1.559
C2–H			1.087	1.078	1.094	1.082	1.104	1.093	2.441	2.411
S–Rh–C2			25.5	26.8			93.9	92.3		
S–Rh–P			92.3	91.8			88.7	86.7		
Rh–S–C4			120.0	126.7			109.2	108.6		
Rh–C2–C3			128.5	125.1	72.2	73.4	131.4	131.7	130.1	129.1
C2–C3–C4	113.3	113.7	113.6	114.0	112.1	112.7	129.1	129.7	115.9	115.6
C3–C4–C5	113.3	113.7	113.6	114.0	115.1	115.1	125.7	127.4	113.7	114.1
C2–Rh–H					20.6	21.3			84.3	83.6
P–Rh–C2–S					198.5	192.3			253.9	263.7

while in the η^1 coordination and the η^2 coordination complexes it is equal to one. The six-membered ring adopts a planar geometry (**3** in Fig. 2). The oxidative addition product **4** is the result of the oxidative addition of the C2–H bond to the rhodium. Again, the cleavage of the bond is indisputable from the long C2–H distance of around 2.4 Å. As in complex **3**, the formal oxidation state of the metal in **4** is equal to three.

Transition states **6** and **7** connecting, respectively, **1** to **3** and **2** to **4** have also been computed at the IMOMM level. Some relevant parameters of each of these are reported in Table 2 and the geometries are shown in Fig. 3.

Transition state **6** is the result of thiophene rotation in its molecular plane in order to reduce the Rh–C2 distance and break the C2–S bond. The thiophene molecule is quite perpendicular to the Rh–S–C2 plane. C2 loses a part of its sp^2 character to become partially sp^3. The S–C2 bond length in **6** (1.857 Å) is not so different from its value in the initial complex **1** (1.822 Å) and the Rh–C2 bond length in **6** (2.257 Å) is closer to its value in the final insertion complex **3** (2.031 Å). The formation of the Rh–C2 bond is thus more advanced than the breaking of the S–C2 bond in transition state **6**.

To reach transition state **7**, the Rh–C2 distance is slightly shortened from complex **2**. The thiophene molecule is tilted because of its rotation around the Rh–C2 axis in order to bring the hydrogen atom bonded to C2 close to the Rh atom.

Table 2 Selected geometrical parameters (in Å and °) obtained from the IMOMM(B3LYP:MM3) optimization of transition states **6** and **7**. Previously reported pure QM values[42] are presented for comparison. X is the centroid of the Cp* ring

	6		**7**	
	Pure QM	QM/MM	Pure QM	QM/MM
Rh–S	3.206	3.246	3.485	3.469
Rh–C2	2.196	2.257	2.113	2.095
Rh–C3	2.716	2.815	3.206	3.140
S–C2	1.884	1.857	1.867	1.852
Rh–H	2.774	2.696	1.671	1.641
S–Rh–C2	34.9	33.7		
S–Rh–P	84.0	81.2		
P–Rh–X	128.9	130.4	130.4	131.2

The formation of the hydride ligand is quite advanced because of the similar values of the Rh–H bond in **7** (1.641 Å) and in **4** (1.559 Å).

Similarly to what was observed for the local minima of the reaction profile, it can be seen in Table 2 that there is an overall good agreement between the computed geometries of the transition states at the IMOMM and at the full QM levels.[42]

Analysis of the energetics

It has just been shown that the IMOMM geometry optimization with a small QM region yields geometries that are very similar to those of the QM calculation on the full system. In order to evaluate the quality of the results one must, however, also consider the relative energies. These are summarized in Fig. 4. For each reaction step, the energy corresponding to the IMOMM calculations just presented (italics) and the previously reported QM calculations[42] (bold) are given. A third value is added, corresponding to the pure QM calculation on the model system [RhCp(PH_3) + thiophene], because it will be used in the analysis that follows.

The first remarkable result from Fig. 4 is that the good agreement between the optimized IMOMM and full QM geometries is not conserved in the case of relative energies, with discrepancies of up to 10.7 kcal mol^{-1} in the step from **1** to **3**. In a more detailed analysis, it can be noticed that the agreement is better in the upper part of the diagram, with an

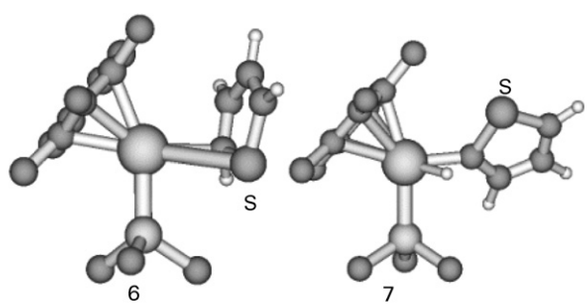

Fig. 3 Optimized IMOMM geometries of the transition states **6** and **7** connecting, respectively, **1** to the C–S bond activation product **3** and **2** to the C–H bond activation product **4**.

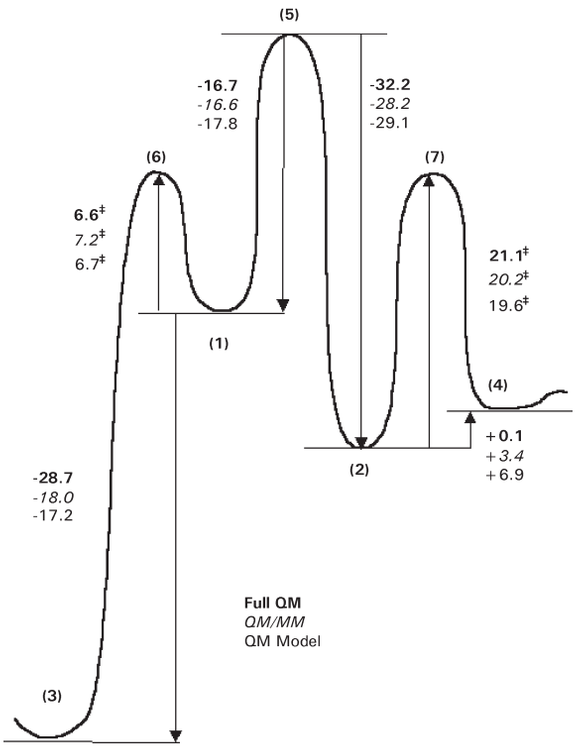

Fig. 4 Computed energies in kcal mol^{-1}. In bold are the pure QM calculations on the full systems,[42] in italics the QM/MM calculations, and in plain type the QM calculations on the model systems. The numbers in parentheses are defined in the text.

actually very good agreement (0.1 kcal mol^{-1} difference) for the transformation from **5** to **1**. It is in the lower part of the diagram where the agreement is the worst. When the thiophene ring is broken to produce the metallacycle (**1** to **3**), or when one H bonded to the C2 of thiophene migrates to the Rh atom (**2** to **4**), the agreement is poor. In these cases the IMOMM method underestimates the binding. The origin of the difference between the two parts of the diagram can be traced to the formal oxidation state of the central rhodium atom. In the upper part of the diagram the rhodium oxidation state is equal to one while in the lower part it is equal to three. The IMOMM method with this QM/MM partition thus does not seem appropriate to describe the energetics of processes involving a change of oxidation state, at least in this particular system. The fact that the geometries are better described than the energies could suggest also the alternative of carrying out full QM calculations on optimized QM/MM geometries.[58] For the step **1** to **3**, which shows the largest difference between the IMOMM and the full QM calculations we have performed such a calculation. The full QM energy from the step **1** to **3** using the related IMOMM geometry is −26.1 kcal mol^{-1} to be compared with −28.7 kcal mol^{-1}. So, this scheme of computation improves significantly the reliability of the results. However, even if in some cases the computed IMOMM energetics are not sufficiently reliable, these results on the full system can be used, together with the QM results and a set of QM results computed for the model system $RhCp(PH_3)$ + thiophene, to evaluate the relative weight of steric and electronic contributions of atoms in the MM region, which in this case are the methyl substituents of both phosphine and cyclopentadienyl.

Fig. 4 also reports the energies of the transition states. The results at all computational levels agree that the breaking of the S–C2 bond through transition state **6** has a significantly lower barrier than the breaking of the C2–H bond through transition state **7**. The discrepancies between IMOMM and full QM follow trends similar to the local minima, but the numerical dispersion is much smaller in the case of transition states. The largest difference is in fact 1.5 kcal mol^{-1} for the energy difference between **2** and **7**. Because of this, in the following we will concentrate on the relative energies of the local minima of the reaction pathway.

Quantification of steric and electronic effects

The type of analysis we are going to carry out is actually quite simple and similar analyses have been previously reported for QM/MM calculations on other systems.[49] The assumptions are that the full QM calculation on the whole system describes correctly the experimental behavior, including the methyl groups, and that the QM/MM calculation describes only the steric effects of the methyls, leaving out their electronic effects. From this, it follows that the total effect of the methyls on a particular reaction step can be computed by subtracting the QM energy of the model system from the QM energy of the whole system and that their steric effect can be obtained by subtracting the QM energy of the model system from the IMOMM energy of the full system. The electronic effect will then simply be computed as the difference between total effect and steric effect. This simple analysis has been applied to obtain the results presented in Table 3.

The results are quite informative. Steric effects are destabilizing (positive sign) for the initial approach of thiophene to the metal, either when going to η^1 (**1**) or to η^2 (**2**), as one would expect from the interaction between two separate fragments. The repulsion is, however, always small, with a maximum of 1.2 kcal mol^{-1}. On the contrary, steric effects are stabilizing in the oxidative addition reactions. This result can seem surprising, taking into consideration that oxidative addition involves an increase in the rhodium coordination number, but it can be understood when looking at the optimized geometries in Fig. 2. The oxidative addition products, **3** and **4**, have the metal in the thiophene plane and this is a sterically more favorable situation than having it in a perpendicular orientation, as was the case in **1** and **2**. Steric effects, therefore, make the initial approach between the reactants more difficult, but then favor the evolution of the reaction towards the final oxidative addition products.

The analysis of electronic effects is also interesting. The effect is very small (−0.1 kcal mol^{-1}) in the case of the η^1 approach leading to **1**. The stability of this complex is based on the donation from a sulfur free electron pair to the metal, which is not very sensitive to the electronic effects of the methyls. The effect of the methyl substituents is, on the other hand, more significant (−4.0 kcal mol^{-1}) for the formation of the η^2 intermediate **2**. In this case, coordination of the C=C double bond to the metal is likely to have important donation and back-donation contributions. The presence of an important back-donation from the metal seems therefore to increase sensitivity to the presence of the methyls. The oxidative addition process is also very sensitive to electronic effects, as expected from the change in oxidation number. It is nevertheless worth noticing that the largest effect (−10.7 kcal mol^{-1}) is observed in the formation of the 6-membered cycle in complex **3**. In this case, the rhodium is likely participating in electron delocalization through the ring.

Table 3 Energetic effect (kcal mol^{-1}) of the methyl substituents on each reaction step and its decomposition into steric and electronic contributions

	5→1	**5→2**	**1→3**	**2→4**
Total	+1.1	−3.1	−11.5	−6.8
Steric	+1.2	+0.9	−0.8	−3.5
Electronic	−0.1	−4.0	−10.7	−3.3

Effects of each ligand on the C–S oxidative addition

In the previous section, we have been able to analyze the importance of the joint effect of the methyl groups in both the cyclopentadienyl and phosphine ligands and discovered that in some cases it was quite significant. The analysis can be taken one step further and the effects of the two ligands, phosphine and cyclopentadienyl, can be evaluated separately. We have studied this aspect only for one particular aspect, the binding energy of thiophene in complex **3**, because the step going from **1** to **3** happens to have the largest substituent effect.

To check the nature of the effect of the methyl groups, we have performed two additional computations on these complexes. The two new molecular systems, shown in Fig. 5, are built as follows. Starting from the whole system, in one case the methyl groups of the phosphine part are replaced by three hydrogen atoms, this is Cp^*RhPH_3. In the other model, the methyl groups of the Cp* moiety are replaced by hydrogens. This is the $CpRhPMe_3$ model.

The computed exothermicity for the step from **5** to **3** is -37.6 kcal mol^{-1} for the $CpRhPMe_3$ model and -38.0 kcal mol^{-1} for the Cp^*RhPH_3 model. Both values happen to be intermediate between those of the smaller $CpRhPH_3$ model with no methyls (-35.1 kcal mol^{-1}) and the larger Cp^*RhPMe_3 system, with methyls on both ligands (-45.4 kcal mol^{-1}). The effect of the methyl groups in both ligands appears to be additive. The total energy difference associated with the replacement of hydrogens by methyls is 10.3 kcal mol^{-1}, the effect of placing methyls on the cyclopentadienyl is 7.4 kcal mol^{-1} and the effect of putting them on the phosphine is 7.8 kcal mol^{-1}. Furthermore, the effect of both ligands is very similar. Therefore, in the reaction steps where the electronic effects must be included, both ligands will have to be fully considered and the full system will have to be computed at a QM level.

Conclusions

The application of the hybrid QM/MM method IMOMM to thiophene activation by Cp^*RhPMe_3 shows that the proposed QM/MM partition, using $CpRhPH_3$ for the QM region, provides a good description of the optimized geometries. This description is, however, too inaccurate for the energetics of some reaction steps, in particular those where there is a change in the formal oxidation state of the metal atom.

The quantification of the effect of the methyl groups in both ligands and its separation into steric and electronic effects shows the general trends operating in the different reaction steps. In particular, it is shown that steric effects are destabilizing in the initial approach between thiophene and complex, but become stabilizing when going to the oxidative addition products. Sensitivity to electronic effects is especially high in the steps where the back-donation from the metal to the thiophene derivative is important and they are always in favor of the activation reaction for the case of the electron-donor methyl groups. It has finally been shown that the effects of methyl substituents in both the phosphine and cyclopentadienyl ligands have similar weights. The combination of pure QM with QM/MM calculations appears as a useful tool to analyze and quantify electronic and steric effects in a catalytic cycle.

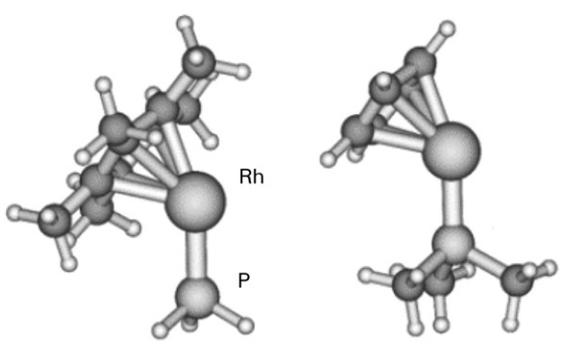

Fig. 5 The Cp^*RhPH_3 (left) and the $CpRhPMe_3$ (right) models.

Acknowledgements

Research partially supported by the Improving the Human Potential Program, Access to Research Infrastructures, under contract HPRI-1999-CT-00071 "Access to CESCA and CEPBA Large Scale Facilities" established between the European Community and CESCA-CEPBA. Financial support is also acknowledged from the Spanish DGI (project No. BQU2002-04110-CO2-02) and the Catalan DURSI (project No. 2001 SGR00179). FM also thanks DURSI for support.

References

1 H. Topsøe, B. Clausen and F. E. Massoth, in Hydrotreating Catalysis, *Catalysis: Science and Technology*, eds. J. R. Anderson and M. Boudart, Springer-Verlag, Berlin, 1996, vol. 11, p. 1.
2 T. C. Ho, *Catal. Rev.*, 1998, **30**, 117.
3 P. T. Vasudevan and J. L. G. Fierro, *Catal. Rev. Sci. Eng.*, 1996, **38**, 161.
4 R. Shafi and G. J. Hutchings, *Catal. Today*, 2000, **59**, 423.
5 B. C. Gates and H. Topsøe, *Polyhedron*, 1997, **16**, 3213.
6 M. V. Landau, *Catal. Today*, 1991, **10**, 489.
7 O. Sørensen, B. J. Clausen, R. Candia and H. Topsøe, *Appl. Catal.*, 1985, **13**, 363.
8 P. C. H. Mitchell, D. A. Green, E. Payen, J. Tomkinson and S. F. Parker, *Phys. Chem. Chem. Phys.*, 1999, **1**, 3387.
9 T. L. Tarbuck, K. M. McCrea, J. W. Logan, J. L. Heiser and M. E. Bussel, *J. Phys. Chem. B*, 1998, **102**, 7845.
10 P. Mills, S. Korlann, M. E. Bussell, M. A. Reynolds, M. V. Ovchinnikov, R. J. Angelici, C. Stinner, T. Weber and R. Prins, *J. Phys. Chem. A*, 2001, **105**, 4418.
11 A. Griboval, P. Blanchard, E. Payen, M. Fournier, J. L. Dubois and J. R. Bernard, *Appl. Catal., A*, 2001, **217**, 173.
12 G. Plazenet, S. Cristol, J. F. Paul, E. Payen and J. Lynch, *Phys. Chem. Chem. Phys.*, 2001, **3**, 246.
13 J. F. Paul and E. Payen, *J. Phys. Chem. B*, 2003, **107**, 4057.
14 J. A. Rodriguez, *J. Phys. Chem. B*, 1997, **101**, 7524.
15 H. Toulhoat, P. Raybaud, S. Kasztelan, G. Kresse and J. Hafner, *Catal. Today*, 1999, **50**, 629.
16 O. Maresca, A. Allouche, J. P. Aycard, M. Rajzmann, F. Hutschka and S. Clémendot, *J. Mol. Struct. (THEOCHEM)*, 2000, **505**, 81.
17 A. Ionescu, A. Allouche, J. P. Aycard, M. Rajzmann and F. Hutchka, *J. Phys. Chem. B*, 2002, **106**, 9359.
18 M. Grillo and P. Sautet, *J. Mol. Catal. A: Chem.*, 2001, **174**, 239.
19 J. Jiao, Y.-W. Li, B. Delmon and J.-F. Hallet, *J. Am. Chem. Soc.*, 2001, **123**, 7334.
20 S. Harris, *Polyhedron*, 1997, **16**, 3219.
21 R. J. Angelici, *Organometallics*, 2001, **20**, 1259.
22 C. Bianchini and A. Meli, *Acc. Chem. Res.*, 1998, **31**, 109.
23 C. Bianchini, A. Meli, S. Monetti, W. Oberhauser, F. Vizza, V. Herrera, A. Fuentes and R. A. Sanchez-Delgado, *J. Am. Chem. Soc.*, 1999, **121**, 7071.
24 J. B. Chen and R. J. Angelici, *Coord. Chem. Rev.*, 2000, **206–207**, 63.
25 M. A. Reynolds, I. A. Guzei and R. J. Angelici, *J. Am. Chem. Soc.*, 2002, **124**, 1689.
26 M. A. Reynolds, I. A. Guzei and R. J. Angelici, *Inorg. Chem.*, 2003, **42**, 2191.
27 P. A. Vecchi, A. Ellern and R. J. Angelici, *J. Am. Chem. Soc.*, 2003, **125**, 2064.
28 C. Bianchini, D. Masi, A. Meli, M. Peruzzini, F. Vizza and F. Zanobini, *Organometallics*, 1998, **17**, 2495.
29 D. G. Churchill, B. M. Bridgewater and G. Parkin, *J. Am. Chem. Soc.*, 2000, **122**, 178.
30 A. W. Myers, W. D. Jones and S. M. McClements, *J. Am. Chem. Soc.*, 1995, **117**, 11 704.
31 A. W. Myers and W. D. Jones, *Organometallics*, 1996, **15**, 2905.

32 M. Hernandez, G. Mirairo, A. Arevalo, S. Bernes, J. J. Garcia, C. Lopez, P. M. Maitlis and F. del Rio, *Organometallics*, 2001, **20**, 4061.
33 D. A. Vicic, A. W. Myers and W. D. Jones, *Organometallics*, 1997, **16**, 2751.
34 D. A. Vicic and W. D. Jones, *Organometallics*, 1999, **18**, 134.
35 M. Paneque, S. Taboada and E. Carmona, *Organometallics*, 1996, **15**, 2678.
36 M. Paneque, P. J. Perez, A. Pizzano, M. L. Poveda, S. Taboada, M. Trujillo and E. Carmona, *Organometallics*, 1999, **18**, 4304.
37 M. Paneque, M. L. Poveda, V. Salazar, E. Carmona and C. Ruiz-Valero, *Inorg. Chim. Acta*, 2003, **345**, 367.
38 (*a*) W. D. Jones, D. A. Vicic, R. M. Chin, J. H. Roache and A. W. Myers, *Polyhedron*, 1997, **16**, 3115; (*b*) D. A. Vicic and W. D. Jones, *J. Am. Chem. Soc.*, 1999, **121**, 7606.
39 (*a*) H. Ki, K. Yu, E. J. Watson, K. L. Virkaitis, J. S. D'Acchioli, G. B. Carpenter, D. A. Sweigart, P. T. Czech, K. R. Overly and F. Coughlin, *Organometallics*, 2002, **21**, 1262; (*b*) K. Yu, H. Li, E. J. Watson, K. L. Virkaitis, G. B. Carpenter and D. A. Sweigart, *Organometallics*, 2001, **20**, 3550.
40 L. Dong, S. B. Duckett, K. F. Ohman and W. D. Jones, *J. Am. Chem. Soc.*, 1992, **114**, 151.
41 A. L. Sargent, E. P. Titus, C. G. Riordan, A. L. Rheingold and P. Ge, *Inorg. Chem.*, 1996, **35**, 7095.
42 A. L. Sargent and E. P. Titus, *Organometallics*, 1998, **17**, 65.
43 *Computational Modeling of Homogeneous Catalysis*, eds. F. Maseras and A. Lledós, Kluwer, Dordrecht, 2002.
44 *Computational Organometallic Chemistry*, T. R. Cundari, Marcel Dekker, New York, 2001.
45 F. Maseras and K. Morokuma, *J. Comput. Chem.*, 1995, **9**, 1170.
46 G. Ujaque, F. Maseras and A. Lledos, *J. Am. Chem. Soc.*, 1999, **121**, 1317.
47 F. Maseras, *Chem. Commun.*, 2000, 1821.
48 P. M. Nave, M. Draganjac, B. Ward, A. W. Cordes, T. M. Barclay, T. R. Cundari, J. J. Carbó and F. Maseras, *Inorg. Chim. Acta*, 2001, **316**, 13.
49 G. Barea, F. Maseras, Y. Jean and A. Lledós, *Inorg. Chem.*, 1996, **35**, 6401.
50 M. J. Frisch, G. W. Trucks, H. B. Schlegel, P. M. W. Gill, B. G. Johnson, M. W. Wong, J. B. Foresman, M. A. Robb, M. Head-Gordon, E. S. Replogle, R. Gomperts, J. L. Andres, K. Raghavachari, J. S. Binkley, C. Gonzalez, R. L. Martin, D. J. Fox, D. J. Defrees, J. Baker, J. P. P. Stewart and J. A. Pople, *Gaussian 92/DFT*, Gaussian, Inc., Pittsburgh, PA, 1993.
51 N. L. Allinger, *mm3(92)*, Quantum Chemistry Program Exchange, Bloomington, IN, 1992.
52 (*a*) C. Lee, W. Yang and R. G. Parr, *Phys. Rev. B*, 1988, **37**, 785; (*b*) A. D. Becke, *J. Chem. Phys.*, 1993, **98**, 5648; (*c*) P. J. Stephens, F. J. Delvin, C. F. Chabalowski and M. J. Frisch, *J. Phys. Chem.*, 1994, **98**, 11 623.
53 P. J. Hay and W. R. Wadt, *J. Chem. Phys.*, 1985, **82**, 270.
54 W. R. Wadt and P. J. Hay, *J. Chem. Phys.*, 1985, **82**, 284.
55 W. J. Hehre, R. Ditchfield and J. A. Pople, *J. Chem. Phys.*, 1972, **56**, 2257.
56 N. L. Allinger, Y. H. Yuh and J. H. Lii, *J. Am. Chem. Soc.*, 1989, **111**, 8551.
57 A. K. Rappé, C. J. Casewit, K. S. Colwell, W. A. Goddard III and W. M. Skiff, *J. Am. Chem. Soc.*, 1992, **114**, 10 024.
58 E. Bustelo, J. J. Carbó, A. Lledós, K. Mereiter, M. C. Puerta and P. Valerga, *J. Am. Chem. Soc.*, 2003, **125**, 3311.